Response calculations based on an independent particle system with the exact one-particle density matrix: Excitation energies

K. J. H. Giesbertz, O. V. Gritsenko, and E. J. Baerends

Additional information on J. Chem. Phys.

Response calculations based on an independent particle system with the exact one-particle density matrix: Excitation energies

K. J. H. Giesbertz,[1,2,3] O. V. Gritsenko,[2,3] and E. J. Baerends[2,3,4,a)]

[1]*Nanoscience Center, P.O. Box 35, 40014 University of Jyväskylä, Finland*
[2]*Theoretical Chemistry, VU University, De Boelelaan 1083, 1081 HV Amsterdam, The Netherlands*
[3]*WCU Program, Department of Chemistry, Pohang University of Science and Technology, Pohang, South Korea*
[4]*Chemistry Department, Faculty of Science, King Abdulaziz University, Jeddah 21589, Saudi Arabia*

Adiabatic response time-dependent density functional theory (TDDFT) suffers from the restriction to basically an occupied $\rightarrow$ virtual single excitation formulation. Adiabatic time-dependent density matrix functional theory allows to break away from this restriction. Problematic excitations for TDDFT, viz. bonding-antibonding, double, charge transfer, and higher excitations, are calculated along the bond-dissociation coordinate of the prototype molecules H_2 and HeH^+ using the recently developed adiabatic linear response phase-including (PI) natural orbital theory (PINO). The possibility to systematically increase the scope of the calculation from excitations out of (strongly) occupied into weakly occupied ("virtual") natural orbitals to larger ranges of excitations is explored. The quality of the PINO response calculations is already much improved over TDDFT even when the severest restriction is made, to virtually the size of the TDDFT diagonalization problem (only single excitation out of occupied orbitals plus all diagonal doubles). Further marked improvement is obtained with moderate extension to allow for excitation out of the lumo and lumo+1, which become fractionally occupied in particular at longer distances due to left-right correlation effects. In the second place the interpretation of density matrix response calculations is elucidated. The one-particle reduced density matrix response for an excitation is related to the transition density matrix to the corresponding excited state. The interpretation of the transition density matrix in terms of the familiar excitation character (single excitations, double excitations of various types, etc.) is detailed. The adiabatic PINO theory is shown to successfully resolve the problematic cases of adiabatic TDDFT when it uses a proper PI orbital functional such as the PILS functional. © 2012 American Institute of Physics. [http://dx.doi.org/10.1063/1.3687344]

I. INTRODUCTION

The time-development of a system subject to a time-dependent perturbation results in time-dependence of properties such as the electron density and the full one-particle reduced density matrix (1RDM). These properties exhibit diverging responses at frequencies of the perturbation corresponding to excitation energies of the system. This effect is the basis of response theory based determination of the excitation energies. Time-dependent density functional (response) theory (TDDFT) uses the response of the electron density (diagonal of the 1RDM). Although typically quite successful for low-lying excitations at equilibrium geometry, it has in its customary adiabatic formulation severe shortcomings for many types of excitations: diagonal double excitations (typically $(homo)^2 \rightarrow (lumo)^2$, see Refs. [1–4]), off-diagonal double excitations (excitation to two different virtuals) occurring in many excited states above the very lowest ones,[3–5] bonding orbital to antibonding orbital (bond breaking) excitations,[6,7] and charge transfer (CT) excitations.[8] It is known that these deficiencies stem from the use of the adiabatic approximation, and could in principle be solved by the application of

frequency dependent kernels. These, however, are not available, and would also make the calculations much more expensive. We will demonstrate in this paper that using time-dependent one-body reduced density matrix functional theory (TD1MFT) (Refs. [3], [4], [9], and [10]) in the adiabatic approximation offers a formulation of response theory that has important advantages. It can essentially solve all the problematic TDDFT cases mentioned above.

In TDDFT the density and its time-dependent response are described by the Kohn-Sham (KS) spinorbitals which have integer (1 or 0) occupations. Because of the constant integer occupations of the time-dependent KS orbitals, only $n_{occ} \times n_{virt}$ occupied-virtual density matrix elements $\delta\gamma_{ia}(\omega)$, $i \leq N$, $a > N$ contribute to the response of the density $\delta\rho(\omega)$ to the frequency-dependent change of the external potential $\delta v(\omega)$. These elements represent single excitations of the ground-state determinant of the KS system. One can say that the density response, the key quantity of the response TDDFT, has a "single-excitation" structure. Due to this structure, only $n_{occ} \times n_{virt}$ single-electron excitations can be determined from the response equations in adiabatic response TDDFT.[11] Apparently, double excitations cannot be described in this approach,[1,2] and a striking example of this failure is the lowest $^1\Sigma_g^+$ excitation of H_2, which is absent in the

adiabatic TDDFT calculations.[3,4] Furthermore, it is a general trend that TDDFT produces reasonable excitation energies ω_α when the Kohn-Sham orbital energy difference $\omega_\alpha^s = \epsilon_a - \epsilon_i$ is already a good first approximation, which is often the case for single excitations in compact molecules or in compact molecular fragments.[12,13] The cases in which the ω_α^s estimate fails are also, as a rule, the problematic TDDFT cases. Examples are the vanishing energy of a single excitation in a bonding-antibonding orbital pair, such as the $1\sigma_g \rightarrow 1\sigma_u$ excitation to the lowest $^1\Sigma_u^+$ state (the B state) in the stretched H_2 molecule,[6,7] and the much too low long-range CT excitations[8,14] obtained with the current adiabatic TDDFT. In both cases the divergence of the exchange-correlation (xc) kernel f_{xc} of TDDFT is required in the long-range limit in order to obtain the correct ω_α,[6,12,15] while the functions f_{xc} of standard adiabatic local density (ALDA) and generalized gradient (AGGA) approximations remain finite.

The 1RDM can be written in its spectral representation as

$$\gamma(\boldsymbol{x}, \boldsymbol{x}'; t) := \langle \Psi | \hat{\psi}_H^\dagger(\boldsymbol{x}'t) \hat{\psi}_H(\boldsymbol{x}t) | \Psi \rangle$$
$$= \sum_k n_k(t) \phi_k(\boldsymbol{x}t) \phi_k^*(\boldsymbol{x}'t), \qquad (1)$$

where the eigenfunctions, $\phi_k(\boldsymbol{x}t)$, are called the natural orbitals (NOs) and acquire fractional occupations $0 \leq n_k(t) \leq 1$ due to the Coulomb electron correlation. Note that Eq. (1) does not define the phases of the NOs, since we can multiply the NOs with an arbitrary phase factor, $e^{i\beta(t)}$ which cancels in the spectral expansion. The response $\delta\gamma(\omega)$, the key quantity of the response TD1MFT, has a richer structure than the density response. It involves in principle the matrix elements $\delta\gamma_{kl}(\omega)$ of all (fractionally occupied) NOs. We will see that the responses in these matrix elements faithfully represent single and double excitations. The theory does not rely on a splitting of the matrix to be diagonalized (representing essentially the inverse of the response function) into orbital energy differences and a coupling part, as is the case in TDDFT, and it does not require diverging constituents to describe excitations in stretched H_2 and CT excitations.[4]

The latest generation of 1MFT functionals describe fairly accurately the molecular ground states. This holds for the equilibrium geometry and bond dissociation energy[16–20] as well as for the energy curves along bond dissociation coordinates.[21,22] This success opens the road to the correct description with adiabatic TD1MFT of the excited state energy surfaces for the above mentioned TDDFT failure cases. However, a serious obstacle is the fact, that with approximate explicit functionals of γ for the electron-electron interaction energy, $W[\gamma]$, as well as with implicit functionals of γ and explicit functionals of the NOs and their occupations $W[\{\phi_k, n_k\}]$, which do not depend on possible NO phases, we inevitably obtain a zero response of the NO occupations $\delta n_k(\omega) = \delta\gamma_{kk}(\omega) = 0$ in the standard adiabatic approximation.[4,10,23,24] This artifact impairs calculated excitation energies, especially for double excitations. This problem has been solved recently by extending the TD1MFT with variables that describe some 2-matrix information. These can be treated as the phases of the one-particle states of the theory, which are the NOs, hence the name phase-including NO (PINO) response theory.[25–27]

In the present paper the PINO response theory is applied to calculation of excitation energies along the bond dissociation coordinates of the prototype molecules H_2 and HeH^+. The calculated excitations include all the TDDFT failure cases. In Sec. II the PINO response theory is summarized and the matrix diagonalization is derived that in the adiabatic approximation of the PINO theory affords the excitation energies as eigenvalues and the corresponding vectors of responses of the density matrix elements as eigenvectors. In Sec. III the density matrix—density matrix response function is analyzed. It can be related, in the Lehmann representation, to the transition density matrices for the excited states of the system. This allows a relation to be established between the eigenvector of the diagonalization corresponding to an excitation and the transition density matrix of the corresponding excited state. The advantage over TDDFT is that the response vector is not limited to an occupied-virtual structure, but more general responses $\delta\gamma_{pq}$ appear, where p, q can refer to both occupied and unoccupied NOs. [We call the first N (usually strongly) occupied NOs the "occupied" NOs and the remaining (usually weakly occupied) ones the "virtual" NOs.] In Sec. IV the physical meaning of the 1RDM response corresponding to an excited state Ψ_α is analyzed from its relation to the transition density matrices $\Delta\boldsymbol{\gamma}^R(\alpha)$ belonging to the state Ψ_α with excitation energy ω_α. The transition density matrix is defined as $\Delta\gamma^R(\alpha|1, 1')$ $:= N \int \Psi_\alpha(1, 2, \ldots, N) \Psi_0^*(1', 2, \ldots, N) \, d2 \cdots dN$. The ground state Ψ_0 and the excited states Ψ_α are supposed to be expanded in determinants in the NO basis, and the contributions to $\Delta\gamma^R(\alpha)$ from the matrix elements between basic determinants can be easily evaluated with the Slater-Condon rules for determinantal matrix elements. Ψ_0 can either be well approximated with the reference determinant Φ_0 built from the first N (strongly occupied) NOs, or it will have, in strong correlation cases, a significant admixture of a diagonal double excitation, usually of the type $(\text{homo})^2 \rightarrow (\text{lumo})^2$. An examination of the commonly encountered cases for the ground state wavefunction (either single-reference type with one leading determinant or correlated with more determinants contributing) and of the excited state wavefunctions (single-excitation type or important contributions from diagonal double excitations or off-diagonal double excitations) affords a straightforward key to interpret the structures of the response vectors and transition density matrices in terms of single and double excitation character of the electronic transitions. In particular, nonzero $\delta\gamma_{ii} = \delta n_i$ and $\delta\gamma_{aa} = \delta n_a$ contributions signify diagonal double excitation character, $(ii)^2 \rightarrow (aa)^2$. Elements $\delta\gamma_{ia}$ represent single excitations (from occupied i to unoccupied a) and $\delta\gamma_{ab}$ signifies off-diagonal double excitation (to the virtuals a and b). The possibility of this identification is key to the improvement afforded by density matrix response theory compared to TDDFT: all these more general excitation types are covered.

Section V discusses the excitations to $^1\Sigma_u^+$ type along the bond dissociation coordinate of H_2. They demonstrate that the TDDFT problem with bonding to antibonding

excitation is solved with the PINO response theory. In Sec. VI the lowest $^1\Sigma_g^+$ excitations in H_2 are presented. The lowest excited state of this symmetry, the EF state $2^1\Sigma_g^+$, is for a large range of distances an essentially doubly excited state (to $(1\sigma_u)^2$ configuration). The calculations demonstrate that such diagonal double excitations can be accurately calculated. The higher $^1\Sigma_u^+$ and $^1\Sigma_g^+$ states provide examples of important off-diagonal excitation character, which also are obtained accurately. In Sec. VII the lowest CT $^1\Sigma^+$ excitations in HeH^+ are presented. They demonstrate the feasibility of charge transfer transitions in the present scheme.

In principle the matrix diagonalization problem has much higher dimension than in the case of TDDFT. In the latter case it has dimension $n_{occ}n_{virt} \times n_{occ}n_{virt}$. In the TD1MFT (and PINO response theory as well) it has in principle roughly dimension $\frac{1}{2}n^2 \times \frac{1}{2}n^2$, since all matrix elements $\delta\gamma_{pq}$, $p \geq q$ may appear in the response vector (n is the size of the basis set). However, we will see that the size of the problem can be reduced without significant loss of accuracy. The diagonal elements $\delta\gamma_{pp} = \delta n_p$ are always all included (although they can possibly be reduced), since this is only a set of order n. Diagonal double excitations are described by diagonal elements $\delta\gamma_{pp}$ and can therefore always be covered. A matrix element $\delta\gamma_{pq}$ indicates contribution from a single excitation $p \rightarrow q$. With the examples treated in the various sections it is demonstrated that the index p in these matrix elements only needs to run over the occupied orbitals, and maybe over one or two orbitals more (the lumo and lumo + 1) if there are significant off-diagonal double excitations. This effectively reduces the size of the TD1MFT problem to only slightly larger than that of TDDFT. In Sec. VIII the conclusions are drawn.

II. PINO RESPONSE THEORY

In TDDFT the central quantity is the time-dependent density, which is treated with the help of effective one-particle equations through the introduction of the KS non-interacting system with the KS orbitals. In the 1RDM related theories the central quantity is the time-dependent 1RDM of Eq. (1), which immediately yields its eigenfunctions, the natural orbitals, as the natural set of one-particle functions to describe its time-development. In a development very much analogous to the one of TDDFT (Ref. 28) we derive effective one-electron time-dependent Schrödinger type of equations for these orbitals by first considering the action A of the interacting system

$$A := \int_0^T dt \, \langle \Psi(t)|i\partial_t - \hat{H}(t)|\Psi(t)\rangle, \tag{2}$$

($\hat{H}(t)$ is the total time-dependent Hamiltonian) as a functional $A[\{\phi, n\}]$ of the NOs and the NO occupations (ONs). Actually, we have given arguments that one should also introduce into the functional, apart from dependence on the NOs and ONs, a dependence on a set of additional variables, which can conveniently be denoted as the phases of the orbitals. [25,26] The expansion (1) does not fix the phases of the NOs, i.e., with the NO $\phi_k(t)$, the orbital $\varphi_k(t) = \phi_k(t)e^{i\beta_k(t)}$ is also a NO. Our basic states are therefore not just the NOs, but PINOs. To fix the

phases of the orbitals, the stationarity of the action (2) is employed in the PINO theory as a phase-fixing condition. Specifically, the PINO theory postulates that the stationary point of (2)

$$\delta A[\{\not{\pi}, n\}] = i \, \langle \Psi(T)|\delta\Psi(T)\rangle \, [\{\not{\pi}, n\}] \tag{3}$$

is attained with the unique set of PINOs

$$\not{\pi}_k(xt) = \phi_k(xt)e^{i\beta_k(t)}. \tag{4}$$

In Eq. (3) the right-hand side is the remainder from the free boundary at time T. [29] The universal functional $A[\{\not{\pi}, n\}]$ is partitioned as follows:

$$A[\{\not{\pi}, n\}] = A_0[\{\not{\pi}, n\}] - A_{Hxc}[\{\not{\pi}, n\}], \tag{5}$$

where A_0 is the one-electron part

$$A_0 := \int_0^T dt \, \sum_k n_k(t)\langle\not{\pi}_k(t)|i\partial_t - \hat{h}(t)|\not{\pi}_k(t)\rangle \tag{6}$$

and A_{Hxc} is the Hartree-exchange-correlation part dealing with all the two-body effects

$$A_{Hxc}[\{\not{\pi}, n\}] := \int_0^T dt \left\{ \langle \Psi(t)|\hat{W}|\Psi(t)\rangle \right.$$
$$\left. + i \sum_k n_k(t)\langle\not{\pi}_k(t)|\dot{\not{\pi}}_k(t)\rangle - i \langle \Psi(t)|\dot{\Psi}(t)\rangle \right\}, \tag{7}$$

where $\hat{W}$ is the two-electron part of the Hamiltonian. With the additional orthonormality conditions on the PINOs, Eq. (3) turns to

$$\delta A_0 - \delta\mathcal{W} - \sum_{kl} \lambda_{kl}(t)(\langle\not{\pi}_k(t)|\delta\not{\pi}_l(t)\rangle + \langle\delta\not{\pi}_k(t)|\not{\pi}_l(t)\rangle)$$
$$= i \sum_k n_k(T)\langle\not{\pi}_k(T)|\delta\not{\pi}_k(T)\rangle, \tag{8}$$

where

$$\delta\mathcal{W}[\{\not{\pi}, n\}] := \delta A_{Hxc} + i \, \langle \Psi(T)|\delta\Psi(T)\rangle$$
$$- i \sum_k n_k(T)\langle\not{\pi}_k(T)|\delta\not{\pi}_k(T)\rangle. \tag{9}$$

Variation in Eq. (8) with respect to $\not{\pi}_k(xt)$, $\not{\pi}_l^*(xt)$, and $n_k(t)$ with the subsequent elimination of the Lagrange multipliers λ_{kl} from the resultant expressions produces the equation of motion (EOM) for the PINOs (Refs. 25 and 26)

$$\left(\hat{h}(t) + \hat{v}_{Hxc}(t)\right)\not{\pi}_k(xt) = i\partial_t\not{\pi}_k(xt) \tag{10}$$

and the EOM for the PINO occupations

$$i\dot{n}_k(t) = \mathcal{W}_{kk}^\dagger(t) - \mathcal{W}_{kk}(t). \tag{11}$$

The potential $\hat{v}_{Hxc}(t)$ in Eq. (10) is defined in terms of its diagonal matrix elements

$$\langle\not{\pi}_k(t)|\hat{v}_{Hxc}(t)|\not{\pi}_k(t)\rangle := \frac{\partial\mathcal{W}(t)}{\partial n_k(t)} \tag{12}$$

and its off-diagonal matrix elements

$$\langle\not{\pi}_k(t)|\hat{v}_{Hxc}(t)|\not{\pi}_l(t)\rangle := \frac{\mathcal{W}_{kl}^\dagger(t) - \mathcal{W}_{kl}(t)}{n_l(t) - n_k(t)} \quad \forall_{k \neq l}, \tag{13}$$

where

$$\mathcal{W}_{kl}(t) := \int d\boldsymbol{x} \, \frac{\partial \mathcal{W}}{\partial \mathcal{t}_k(\boldsymbol{x}t)} \mathcal{t}_l(\boldsymbol{x}t). \tag{14}$$

In the adiabatic approximation the functional $\mathcal{W}[\{\mathcal{t}, n\}](t)$ is replaced with the functional $W[\{\mathcal{t}, n\}]$ of the static electron-electron interaction energy.

We now proceed to derive equations for the excitation energies using the linear response formalism.[25,26] First consider a time-independent system. The system has stationary solutions for the PINOs of the form

$$\mathcal{t}_k^0(\boldsymbol{x}t) = \mathcal{t}_k(\boldsymbol{x}) e^{-i\epsilon_k t}, \tag{15}$$

where the time-independent PINOs satisfy

$$\left(\hat{h} + \hat{v}_{\text{Hxc}}\right) \mathcal{t}_k(\boldsymbol{x}) = \epsilon_k \mathcal{t}_k(\boldsymbol{x}). \tag{16}$$

Now we apply a time-dependent perturbation to the potential, $\delta\boldsymbol{v}(t)$. The PINOs are now perturbed and we expand the perturbation in them as

$$\mathcal{t}_k(\boldsymbol{x}t) =: e^{-i\epsilon_k t}\left(\mathcal{t}_k(\boldsymbol{x}) + \delta\mathcal{t}_k(\boldsymbol{x}t) + \cdots\right). \tag{17}$$

The perturbation in the NOs, $\delta\mathcal{t}_k(\boldsymbol{x}t)$, is expanded in the stationary time-independent PINOs as

$$\delta\mathcal{t}_k(\boldsymbol{x}t) =: \sum_r \mathcal{t}_r(\boldsymbol{x})\delta U_{rk}(t). \tag{18}$$

Since the PINOs are still NOs, the perturbation in the 1RDM is readily expressed as

$$\delta\gamma_{kl}(t) = \delta n_k(t)\delta_{kl} + (n_l - n_k)\delta U_{kl}(t). \tag{19}$$

Using these expressions for the perturbations, one can derive the frequency dependent response equations. Details of the derivation can be found in Refs. 26 and 27. The results can be summarized as follows. Using the adiabatic approximation, $\mathcal{W} \approx W$, and restricting ourselves to systems with time-reversal symmetry, the frequency-dependent response equations can be cast into the following form:

$$\begin{pmatrix} \omega\boldsymbol{1} & -\boldsymbol{A}^+ \\ -\boldsymbol{D} & \omega\boldsymbol{1} \end{pmatrix}\begin{pmatrix} \boldsymbol{X}(\omega) \\ \boldsymbol{Y}(\omega) \end{pmatrix} = \begin{pmatrix} \boldsymbol{0} \\ \boldsymbol{V}(\omega) \end{pmatrix}. \tag{20}$$

The vectors $\boldsymbol{X}$ and $\boldsymbol{Y}$ collect the perturbations in the PINOs and occupation numbers as

$$\boldsymbol{X}(\omega) := \begin{pmatrix} \delta\boldsymbol{\gamma}^R(\omega) \\ \delta\boldsymbol{n}(\omega) \end{pmatrix}, \quad \boldsymbol{Y}(\omega) := \begin{pmatrix} i\delta\boldsymbol{U}^I(\omega) \\ i\delta\boldsymbol{U}^D(\omega)/2 \end{pmatrix}, \tag{21}$$

where the superscript D means only the diagonal elements. The superscripts R and I indicate the Fourier transforms of the real and imaginary parts respectively, i.e.,

$$f^R(\omega) := \mathcal{F}[\mathfrak{Re} \, f](\omega), \quad f^I(\omega) := \mathcal{F}[\mathfrak{Im} \, f](\omega). \tag{22}$$

The superscripts R and I attached to a matrix (here at $\delta\boldsymbol{\gamma}$ and $\delta\boldsymbol{U}$) denote a vector consisting of only the lower off-diagonal matrix elements ($\delta\gamma_{kl}^R$ and δU_{kl}^R, $k > l$). Due to the assumed time-reversal symmetry, we only need to consider real PINOs, $\mathcal{t}_k(\boldsymbol{x})$, so the potential on the right-hand side of Eq. (20) has only real entries

$$\boldsymbol{V}(\omega) := \begin{pmatrix} \delta\boldsymbol{v}^R(\omega) \\ \delta\boldsymbol{v}^D(\omega)/2 \end{pmatrix}. \tag{23}$$

The matrix on the left-hand side of Eq. (20) is determined by the unperturbed system and is a rather involved quantity. An important ingredient is the response of the two-electron part in the equations, which are given by the coupling matrices

$$K_{kl,ba}^{\mathcal{t}} := \int d\boldsymbol{x} \left(\frac{\partial\left(W_{kl}^\dagger - W_{kl}\right)}{\partial\mathcal{t}_b(\boldsymbol{x})}\mathcal{t}_a(\boldsymbol{x}) - \mathcal{t}_b^*(\boldsymbol{x})\frac{\partial\left(W_{kl}^\dagger - W_{kl}\right)}{\partial\mathcal{t}_a^*(\boldsymbol{x})} \right), \tag{24a}$$

$$K_{kl,a}^n := \frac{\partial\left(W_{kl}^\dagger - W_{kl}\right)}{\partial n_a}, \tag{24b}$$

$$\overline{W}_{k,a} := \frac{\partial^2 W}{\partial n_k \partial n_a}. \tag{24c}$$

The response of the two-electron part is combined with contributions from the one-electron part

$$A_{kl,ba} := (n_b - n_a)(h_{ka}\delta_{bl} - \delta_{ka}h_{bl}) + K_{kl,ba}^{\mathcal{t}}, \tag{25a}$$

$$C_{kl,a} := h_{kl}(\delta_{al} - \delta_{ka}) + K_{kl,a}^n. \tag{25b}$$

Now we define the $\boldsymbol{A}^\pm$ matrices as

$$A_{kl,ba}^\pm := A_{kl,ba} \pm A_{kl,ab}. \tag{26}$$

The submatrix $\boldsymbol{D}$ is defined as a composition of the previously introduced matrices

$$\boldsymbol{D} := \begin{pmatrix} \boldsymbol{N}^{-1}\boldsymbol{A}^-\boldsymbol{N}^{-1} & \boldsymbol{N}^{-1}\boldsymbol{C} \\ \boldsymbol{C}^T\boldsymbol{N}^{-1} & \overline{\boldsymbol{W}} \end{pmatrix}, \tag{27}$$

where $N_{kl,ba} := (n_l - n_k)\delta_{ka}\delta_{bl}$. Equation (20) can be manipulated a bit further to reduce the dimensions by eliminating $\boldsymbol{Y}(\omega)$ from the response equations. After some further manipulations we find[30]

$$\left[\omega^2\boldsymbol{1} - \sqrt{\boldsymbol{A}^+}\boldsymbol{D}\sqrt{\boldsymbol{A}^+}\right](\boldsymbol{A}^+)^{-1/2}\boldsymbol{X}(\omega) = \sqrt{\boldsymbol{A}^+}\boldsymbol{V}(\omega). \tag{28}$$

It is clear that at values of ω which are eigenvalues of the matrix $\sqrt{\boldsymbol{A}^+}\boldsymbol{D}\sqrt{\boldsymbol{A}^+}$ responses may exist even in the absence of a driving field $\boldsymbol{V}(\omega)$. Those eigenvalues must coincide with the "eigenfrequencies" of the system, i.e., its excitation energies. We can also solve for $\boldsymbol{X}(\omega)$ explicitly. Since the matrix on the left-hand side of Eq. (28) is symmetric, it can be inverted. In particular, with the decomposition

$$\sqrt{\boldsymbol{A}^+}\boldsymbol{D}\sqrt{\boldsymbol{A}^+}\,\boldsymbol{F}_k = \omega_k^2\boldsymbol{F}_k, \tag{29}$$

we can solve Eq. (28) for $\boldsymbol{X}(\omega)$ as

$$\boldsymbol{X}(\omega) = \sqrt{\boldsymbol{A}^+}\sum_k \frac{\boldsymbol{F}_k\boldsymbol{F}_k^T}{\omega^2 - \omega_k^2}\sqrt{\boldsymbol{A}^+}\boldsymbol{V}(\omega). \tag{30}$$

This equation connects the responses collected in the vector $\boldsymbol{X}(\omega)$ with the perturbing field $\boldsymbol{V}(\omega)$, i.e., is of the form $\delta\boldsymbol{\gamma} = \boldsymbol{\chi}\,\delta\boldsymbol{v}$, where $\boldsymbol{\chi}$ is the 1RDM-1RDM response function. Therefore, comparing Eq. (30) with the Lehmann representation of the 1RDM-1RDM response function will

enable us to identify the ω_k with the excitation energies and $\sqrt{A^+}F_k/(2\sqrt{\omega_k})$ with the transition 1RDMs, see Sec. III.

III. CONNECTION OF THE 1RDM RESPONSE VECTOR OF AN EXCITED STATE WITH THE TRANSITION DENSITY MATRIX

Excited states are characterized by the transition density matrix connecting the ground and excited states. In this section we will establish the relationship between the calculated responses, as embodied in the $X(\omega)$ (or $F_k(\omega)$), and the transition density matrices. We start with the Lehmann representation of the 1RDM-1RDM response function. Using perturbation theory,[31] the perturbation in the 1RDM, $\delta\gamma(t)$, due to a perturbation in the potential, $\delta v(t)$ can be written as

$$\delta\gamma_{kl}(t) = \int_{-\infty}^{\infty} dt' \sum_{ab} \chi_{kl,ba}(t-t')\,\delta v_{ab}(t'). \quad (31)$$

The retarded response function, $\chi(t-t')$, is defined as

$$\chi_{kl,ba}(t-t') := -i\theta(t-t')\langle\Psi_0|[\hat{\gamma}_{kl}(t), \hat{\gamma}_{ab}(t')]|\Psi_0\rangle, \quad (32)$$

where $\hat{\gamma}(t)$ is the 1RDM operator in the Heisenberg picture with elements $\hat{\gamma}_{kl}(t) = \hat{c}_l^\dagger(t)\hat{c}_k(t)$, and the Heaviside step function is defined as

$$\theta(\tau) = \begin{cases} 1 & \text{for } \tau > 0 \\ 0 & \text{for } \tau < 0. \end{cases} \quad (33)$$

The step function reflects that we have a causal response, i.e., changes in the 1RDM only depend on perturbations in the potential at earlier times. From basic complex analysis, the step function can also be written as

$$\theta(\tau) := -\lim_{\eta\to 0^+} \int_{-\infty}^{\infty} \frac{d\omega}{2\pi i} \frac{e^{-i\omega\tau}}{\omega + i\eta}. \quad (34)$$

Inserting a complete set of states and taking the Fourier transform of Eq. (32), we obtain the frequency dependent 1RDM-1RDM response function (Lehmann representation)

$$\chi(\omega) = \lim_{\eta\to 0^+} \sum_\alpha \left(\frac{\Delta\gamma(\alpha)\otimes\Delta\gamma(\alpha)^\dagger}{\omega - \Omega_\alpha + i\eta} - \frac{\Delta\gamma(\alpha)^\dagger\otimes\Delta\gamma(\alpha)}{\omega + \Omega_\alpha + i\eta} \right), \quad (35)$$

where Ω_α are the excitation energies and the transition 1RDMs are defined as

$$\Delta\gamma_{kl}(\alpha) := \langle\Psi_0|\hat{\gamma}_{kl}|\Psi_\alpha\rangle \quad (36a)$$

and its complex conjugate as

$$\Delta\gamma_{kl}^\dagger(\alpha) := \langle\Psi_0|\hat{\gamma}_{lk}|\Psi_\alpha\rangle^* = \langle\Psi_\alpha|\hat{\gamma}_{kl}|\Psi_0\rangle. \quad (36b)$$

Note that the $i\eta$ terms in the denominator reflect the causality of the retarded response function, i.e., they come from the Fourier transform of the step function (34), contrary to a common belief which attributes their appearance to some unphysical adiabatic switch-on of the perturbation.

Since our response Eq. (30) only deals with the real part of the 1RDM, we actually only need the $\gamma^R\gamma^R$ response

function

$$\chi_{kl,ba}^{RR}(\omega) = \sum_\alpha \Delta\gamma_{kl}^R(\alpha)\Delta\gamma_{ab}^R(\alpha)$$
$$\times \left[\mathcal{P}\frac{2\Omega_\alpha}{\omega^2 - \Omega_\alpha^2} - i\pi(\delta(\omega-\Omega_\alpha) - \delta(\omega+\Omega_\alpha)) \right], \quad (37)$$

where $\mathcal{P}$ indicates the Cauchy principal value. Note that we dropped the complex conjugation, since we assumed time-reversal symmetry, so the eigenstates of the reference system can be chosen to be real. Since we did not take causality into account in our response Eq. (30), we should only compare the principal value part. The only thing we need to keep in mind is that in Eq. (30) the sum only runs over $a \geq b$, whereas in Eq. (31) the sum runs over all a, b. So we need to introduce a factor 1/2 for the off-diagonal elements to make the comparison. Since the diagonal elements of the perturbation already had a factor half in Eq. (23) we can pull it inside the summation of Eq. (30) and find

$$\mathcal{P}\chi^{RR}(\omega) = \sum_\alpha \Delta\gamma^R(\alpha)\otimes\Delta\gamma^R(\alpha)\,\mathcal{P}\frac{2\Omega_\alpha}{\omega^2 - \Omega_\alpha^2}$$
$$= \sum_k \frac{\sqrt{A^+}F_k F_k^T \sqrt{A^+}}{2(\omega^2 - \omega_k^2)}. \quad (38)$$

Since this relation has to hold for every ω, we find that the eigenvalues ω_k from Eq. (29) are exactly the excitation energies Ω_k and that the real part of the transition 1RDMs are related to the eigenvectors F_k as

$$\Delta\gamma^R(\alpha) = \frac{\sqrt{A^+}F_\alpha}{2\sqrt{\Omega_\alpha}}. \quad (39a)$$

The imaginary part of the transition 1RDMs is now readily derived, since the perturbations in the real and imaginary part of the 1RDM are related according to Eq. (20). Using the definitions (21), we find

$$i\Delta\gamma^I(\alpha) = \Omega_\alpha(A^+)^{-1}\Delta\gamma^R(\alpha) = \frac{1}{2}\sqrt{\Omega_\alpha}N(A^+)^{-1/2}F_\alpha. \quad (39b)$$

Another approach to derive this relation would be to write down the $\chi^{IR}(\omega)$ response function and perform a similar analysis as before.

In Sec. IV, Eq. (39) will be used in order to interpret the eigenvectors F_k of Eq. (29), to assign the calculated excitations as well as to rationalize the performance of the restricted response calculations.

IV. CONNECTION OF THE TRANSITION DENSITY MATRIX WITH THE "SINGLE-AND-DOUBLE EXCITATION" CHARACTER OF THE EXCITED STATE

We demonstrate in this section that the TDDMFT response theory is able to represent not only excited states of predominantly singly excited character, but also various types of double excitations. Also charge transfer transitions will be shown to be obtained accurately. At each excitation energy we obtain the corresponding response vector F_k and we

can determine the transition density matrix from Eq. (39). We demonstrate here that the 1RDM responses obtained at the excitation energies afford a representation of transition density matrices for excited states of singly excited and doubly excited character, also from ground states that are not of single-reference type. We assume the wavefunctions of the ground state and excited states are written as linear combinations of determinants based on the NOs as one-electron basis,

$$\Psi_0 = C_0 \Phi_0 + C_i^a \Phi_i^a + C_{ij}^{ab} \Phi_{ij}^{ab} + \ldots, \quad (40)$$

$$\Psi_{\text{exc}} = D_0 \Phi_0 + D_i^a \Phi_i^a + D_{ij}^{ab} \Phi_{ij}^{ab} + \ldots, \quad (41)$$

$i, j, k \ldots \leq N$ are indices running over the N (strongly) occupied NOs, $a, b, c\ldots$ run over the virtual (weakly occupied) NOs. Close to the equilibrium geometry this will typically yield a single-reference picture with the determinant Φ_0 built from the first N (strongly occupied) NOs as leading term, and small coefficients for the singly, doubly, and more highly excited determinants. We will also consider the case where the ground state has multideterminant character, later in this section. If an excited state is of singly excited ($i \to a$) character, the coefficient D_0 will be small and the D_i^a coefficient will be large; if it is of doubly excited ($ij \to ab$) character, D_{ij}^{ab} will be large, etc. The interpretation of $\Delta\boldsymbol{\gamma}^R(\alpha)$ follows immediately by substituting these ground state and excited state wavefunctions in Eq. (36) and using the Slater-Condon rules to evaluate the matrix element. Note that the transition density of Eq. (36) will lead to many determinant-determinant terms,

$$\Delta\gamma(\Phi_1\Phi_2|1, 1') = N \int \Phi_1(1, 2, \ldots, N)$$
$$\times \Phi_2^*(1', 2, \ldots, N) \, d2 \cdots dN. \quad (42)$$

The following rules apply:

- Two equal determinants yield contributions to the diagonal elements $\Delta\gamma_{pp}$ for all p in the determinant

$$N \int C_1 D_1^* \Phi_1(1, 2, \ldots, N) \Phi_1^*(1', 2, \ldots, N) \, d2 \cdots dN$$
$$= \Sigma_{p=1}^N C_1 D_1^* \phi_p(1) \phi_p^*(1'). \quad (43)$$

  So all diagonal terms in the product $\Psi_0 \Psi_{\text{exc}}^*$ (i.e., $C_0 D_0^* \Phi_0 \Phi_0^*$, $C_i^a D_i^{a*} \Phi_i^a \Phi_i^{a*}$, $C_{ij}^{ab} D_{ij}^{ab*} \Phi_{ij}^{ab} \Phi_{ij}^{ab*}$, etc.) will contribute to diagonal $\Delta\gamma_{pp}$ elements if they contain the NO p.

- Two determinants that differ in one function (e.g., Φ_0 and Φ_i^a) yield only one $\Delta\gamma_{pq}$ element, just for the functions in which they differ. For example, for Φ_0 and Φ_i^a,

$$N \int C_0 D_i^{a*} \Phi_0(1, 2, \ldots, N) \Phi_i^{a*}(1', 2, \ldots, N)$$
$$\times d2, d3 \cdots dN = C_0 D_i^{a*} \phi_i(1) \phi_a^*(1'). \quad (44)$$

- Two determinants that differ in two functions yield zero contribution to the $\Delta\gamma$ matrix.

So an $\alpha = (i \to a)$ singly excited state ($D_i^a \approx 1$) from a single-reference ground state ($C_0 \approx 1$) will lead to a single large $\Delta\boldsymbol{\gamma}^R(\alpha)$ matrix element, i.e., $\Delta\gamma_{ia}^R(i \to a) \approx C_0 D_i^a$. This will make such a type of excited state easily recognizable. It is to be noted that at zero excitation energy also a solution will be obtained, which corresponds to the ground state. It will be characterized by all diagonal terms $(\Delta\gamma_{ii}^R)(0) \approx (C_0)^2$, $i = 1 \ldots N$. An excited state with predominant double excitation character, e.g., $(ij \to ab)$ (an off-diagonal double, from the closed shells $(\phi_i)^2$ and $(\phi_j)^2$ to the open shell configuration $(\phi_i)^1(\phi_j)^1(\phi_a)^1(\phi_b)^1$), will probably be at high energy if the ground state is of single-determinant type. If we assume that the same doubly excited configuration is the most important one in the ground state wavefunction, this excited state will be characterized with the largest $\Delta\boldsymbol{\gamma}^R(\alpha)$ matrix elements for $\Delta\boldsymbol{\gamma}_{aa}^R$ and $\Delta\boldsymbol{\gamma}_{bb}^R$, as well as for $\Delta\boldsymbol{\gamma}_{kk}^R$, $k \neq i, j$. In the case of a single-reference type ground state, such doubly excited states will usually not be encountered in the interesting (low-energy) part of the excitation spectrum.

It is of interest to consider the case where a single reference is no longer adequate, i.e., a doubly excited determinant, $(i\bar{i} \to a\bar{a})$, makes an important contribution to the ground state (strong nondynamical correlation). This is of course the case at elongated bond lengths in H_2, where a strong mixing of the $(1\sigma_g)^2$ and $(1\sigma_u)^2$ configurations occurs. More generally, we consider the case that Ψ_0 is approximated with the reference determinant Φ_0 built from the N first (strongly occupied) PINOs plus an admixture of a diagonal double excitation $(\phi_i)^2 \to (\phi_a)^2$, which will usually be from the last strongly occupied NO ($i = N$, the "homo") to the first weakly occupied NO ($a = N + 1$, the "lumo"),

$$\Psi_0 \approx C_0 \Phi_0 + C_{h\bar{h}}^{l\bar{l}} \Phi_{h\bar{h}}^{l\bar{l}}. \quad (45)$$

It can easily be seen that this non-single-reference character of the ground state does not make much difference for singly excited states of $(i \to a)$ type if $i \neq h$ and $a \neq l$. The matrix element in Eq. (36) between $C_0 \Phi_0$ and $D_i^a \Phi_i^a$ will again yield $\Delta\gamma_{ia}^R = C_0 D_i^a$. If the $(\phi_h)^2 \to (\phi_l)^2$ determinant also makes a large contribution to the $(i \to a)$ singly excited state, i.e., the contribution of the configuration with simultaneously $(i \to a)$ and $(\phi_h)^2 \to (\phi_l)^2$ is large in Ψ_{exc}, then also a significant contribution $\Delta\gamma_{ia}^R = C_{h\bar{h}}^{l\bar{l}} D_{h\bar{h},i}^{l\bar{l},a}$ will arise,

$$\Delta\gamma_{ia}^R(\Psi_0(45) \to \Psi_{\text{exc}}(i \to a)) = C_0 D_i^a + C_{h\bar{h}}^{l\bar{l}} D_{h\bar{h},i}^{l\bar{l},a}. \quad (46)$$

The special single excitation $(h \to l)$ between the two orbitals involved in the nondynamical correlation embodied in wavefunction (45), with $\Psi_{\text{exc}} \approx D_h^l \Phi_h^l$, $D_h^l \approx 1$, will have a matrix element (36) of Ψ_{exc} with both Φ_0 and $\Phi_{h\bar{h}}^{l\bar{l}}$, so

$$\Delta\gamma_{hl}^R(\Psi_0(45) \to \Psi_{\text{exc}}(h \to l)) = C_0 D_h^l + C_{h\bar{h}}^{l\bar{l}} D_h^l. \quad (47)$$

So all excited states of single excitation nature are characterized by a single large transition density matrix element $\Delta\gamma_{ia}^R$ (including $\Delta\gamma_{hl}^R$), with corresponding large response vector element.

Of special interest is a possible "double excitation" structure in the 1RDM response. In the case of the ground state

(45), the excitation to the "diagonal doubly excited" state $(\phi_h)^2 \rightarrow (\phi_l)^2$ with $\Psi_{exc} \approx D_0 \Phi_0 + D_{h\bar{h}}^{l\bar{l}} \Phi_{h\bar{h}}^{l\bar{l}} = -C_{h\bar{h}}^{l\bar{l}} \Phi_0 + C_0 \Phi_{h\bar{h}}^{l\bar{l}}$ can be important. This excitation will lead to large diagonal elements

$$\Delta\gamma_{hh}^R = \Delta n_h \approx -C_0 C_{h\bar{h}}^{l\bar{l}}, \quad \Delta\gamma_{ll}^R = \Delta n_l \approx C_{h\bar{h}}^{l\bar{l}} C_0, \quad (48)$$

(note that the contributions to all other $\Delta\gamma_{ii}^R, i \neq h$, arising according to Eq. (43) from the $\langle\Phi_0|\Phi_0\rangle_{2\ldots N}$ and $\langle\Phi_{h\bar{h}}^{l\bar{l}}|\Phi_{h\bar{h}}^{l\bar{l}}\rangle_{2\ldots N}$ integrals, cancel). One obtains $\Delta n_h = 1/2$ and $\Delta n_l = -1/2$ in the case of equal mixing of the two determinants ($C_0 = -C_{h\bar{h}}^{l\bar{l}} = 1/\sqrt{2}$). The ground state will then be characterized by $\Delta n_h = \Delta n_l = +1/2$. For the ground state wavefunction (45) embodying nondynamical correlation, off-diagonal double excitations will be important if they involve ϕ_h and ϕ_l. One possibility is excitation of the two electrons in $(\phi_h)^2$ to $(\phi_l)^1(\phi_a)^1$. The other possibility is an excitation $\phi_i\phi_h$ to $(\phi_l)^2$. A configuration $(\phi_l)^1(\phi_a)^1$ will have zero contribution to the transition density matrix from the Φ_0 component of the ground state, but it has a nonzero contribution from the matrix element with $\Phi_{h\bar{h}}^{l\bar{l}}$, being of single-excitation type with respect to that determinant. The corresponding transition density matrix element will then be

$$\Delta\gamma_{la}^R(\Psi_0(45) \rightarrow \Psi_{exc}(h^2 \rightarrow la)) = C_{h\bar{h}}^{l\bar{l}} D_{h\bar{h}}^{la}. \quad (49)$$

which is significant if the configuration $(\phi_h)^0(\phi_l)^2$ makes an important contribution to the ground state ($C_{h\bar{h}}^{l\bar{l}} \gg 0$). Instead of describing this as an off-diagonal double excitation with respect to Φ_0 we note that a large $\Delta\gamma_{la}^R$ apparently describes a single excitation from the lumo to a higher orbital, which can clearly only be important in the nondynamical correlation case of wavefunction (45), where the lumo becomes occupied. It is covered in the $\Delta\gamma^R$ response vector by extending the range of the i index beyond the homo to include also the lumo. The configuration $\phi_i\phi_h$ to $(\phi_l)^2$ may in the same way be described as a single excitation $\phi_i \rightarrow \phi_h$ with respect to the determinant $\Phi_{h\bar{h}}^{l\bar{l}}$, becoming important when this determinant has significant weight in the ground state wavefunction, i.e., when $C_{h\bar{h}}^{l\bar{l}} \gg 0$. In that case the transition density matrix element becomes

$$\Delta\gamma_{ih}^R(\Psi_0(45) \rightarrow \Psi_{exc}(ih \rightarrow l^2)) = C_{h\bar{h}}^{l\bar{l}} D_{ih}^{l\bar{l}}. \quad (50)$$

The special cases of Eqs. (49) and (50) demonstrate the meaning that can be given to these "virtual → virtual" and "occupied → occupied" type of excitations.

The qualitative analysis of this section shows that, unlike the density response in TDDFT, which is limited to a response vector with only occupied-virtual (ia) elements, giving it an essentially "single-excitation" structure, the 1RDM response displays "single-and-double" excitation structure. Furthermore, the present analysis suggests an efficient strategy for the 1RDM response calculations. One can severely restrict the size of the response calculations retaining only those elements which will attain significant values. We always retain all diagonal elements (occupation number responses Δn_k). This will incorporate possible nondynamical correlation effects as embodied in wavefunction (45) and the double excitations characterized by the occupation number changes of Eq. (48). A first restriction would include only "occupied-

all" elements $\Delta\gamma_{i,a}$, where i runs to h and a runs over the full PINO set. This restricted variant, denoted R0, is roughly equivalent in size to the response TDDFT. In a slightly extended variant, denoted R1, the elements of the R0 variant are augmented with the elements $\Delta\gamma_{la}$, i.e., the homo+1 (lumo) is included in the range of index i. In a further extension we use variant R2, in which the next higher orbital (homo+2) is also included in the range of the first index. We have in this paper not studied any restriction of i within the occupied set or of a within the virtual set, since we have only one occupied orbital. Obviously, in a many-electron system it will be interesting to test restriction of the range of the indices also in the set of occupied and virtual PINOs.

The established "single-and-double" excitation structure of the 1RDM response suggests that time-dependent PINO functional theory could produce single and double excitations already in the adiabatic approximation. This will be demonstrated in Secs. V–VII. Of course, we require an accurate functional which captures the dynamics of the occupation numbers. For singlet two-electron systems, we actually know the exact PINO functional. This is the Löwdin-Shull expression for the total energy of a two-electron system, in which use is made of the finding that the wavefunction in NO basis can be written as a summation over diagonal doubly excited determinants, with the square roots of the occupation numbers as coefficients, each coefficient having positive or negative phase. This energy expression thus depends not only on the NOs and the NO occupation numbers, but also on the additional phase factors which we can introduce as phases of the PINOs. We denote the PINO energy expression obtained in this way as the phase-including Löwdin-Shull functional, PILS

$$W^{PILS} = \frac{1}{2} \sum_{kl} \sqrt{n_k n_l} w_{kkll}, \quad (51)$$

where

$$w_{klba} \equiv \int dx \int dx' \, \pi_k^*(x) \pi_l^*(x') w(x, x') \pi_b(x') \pi_a(x). \quad (52)$$

In ground state calculations similar $\sqrt{n}$-based functionals have been used, but with exchange like integrals w_{kllk} instead of the w_{kkll} of Eq. (52). This is the natural choice in the Müller derivation[32] of the $\sqrt{n}$ functional since it is based on extension of the exchange energy expression. It is one of the two choices in the Buijse-Baerends derivation[33,34] of this functional. With this phase choice the functional is a genuine density matrix functional, not depending on the phase of the NOs. If the orbitals are all real, this does not make any difference in the ground state total energy. However, the phase choice does play a role in the response calculations. The functional with the w_{kllk} phase choice, denoted the density-matrix adaptation of the Löwdin-Shull energy (DMLS functional), indeed leads to complications in response calculations.[25,26] In fact, the seemingly innocuous exchange-like phase choice in this functional leads to disastrous response results if the calculations are pushed to higher accuracy than R2.[27] In Secs. V–VII, we will concentrate on the PILS functional for calculations of the excitation energies in the restricted R0, R1 and R2 variants.

V. APPLICATIONS: POTENTIAL ENERGY CURVES FOR THE $^1\Sigma_u^+$ EXCITED STATES OF H_2

In this section the results of comparative calculations of the potential energy curves for the lowest excited states of the $^1\Sigma_u^+$ symmetry of the H_2 molecule are presented. The potential curves for the lowest four $^1\Sigma_u^+$ states are displayed in Fig. 1. The reference full configuration interaction (FCI) calculations have been performed in the aug-cc-pVTZ basis[35] with the DALTON package.[36]

The ground state of H_2 is characterized with the two-electron bond H–H. It can be roughly described with the expansion (45) where the coefficient C_0 of the configuration $(1\sigma_g)^2$ decreases and the (absolute value of the) coefficient $C_{1\sigma_g 1\sigma_g}^{1\sigma_u 1\sigma_u}$ of the configuration $(1\sigma_u)^2$ increases with R(H–H). The lowest $^1\Sigma_u^+$ state ($B^1\Sigma_u^+$) goes at long distance to an ionic configuration, H_a^+-H_b^- − H_a^--H_b^+, with high energy because of the repulsion between two electrons, which are instantaneously located on the same H atom (in the asymptotic limit of $R \rightarrow \infty$ the lowest $^1\Sigma_u^+$ goes to a covalent state with one H atom in the $1s \rightarrow 2s$ excited state[37]). Near the equilibrium H–H distance, all four $^1\Sigma_u^+$ states are, predominantly, single excitations from the $1\sigma_g$ orbital to orbitals of σ_u type. In the representation of the HF orbitals, the $1^1\Sigma_u^+$
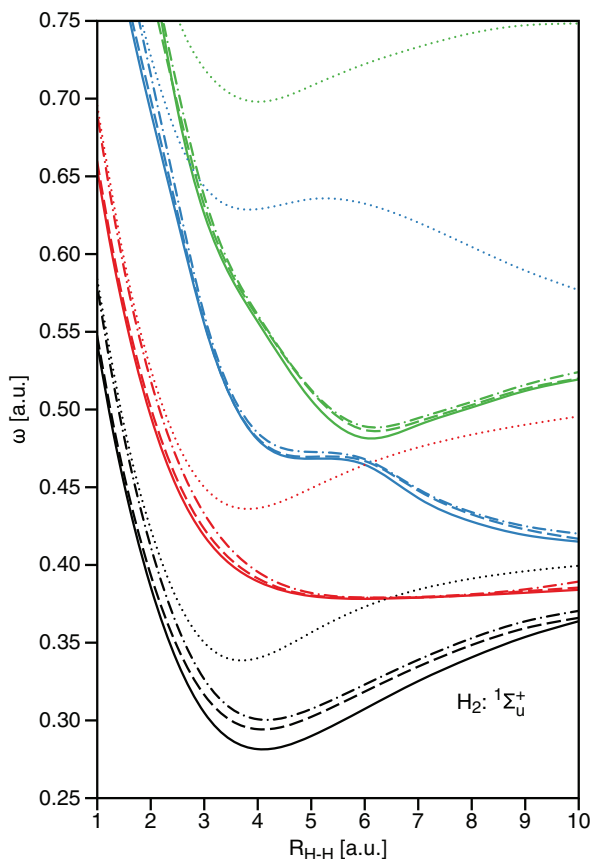

FIG. 1. H_2 $^1\Sigma_u^+$ excitation energies along the bond breaking coordinate calculated exactly (full CI) and with PINO response calculations with the PILS functional. Full CI: solid lines; PILS-R0: dots; PILS-R1: dotted-dash; PILS-R2: dashes. Black, red, blue, green for 1st, 2nd, 3rd, and 4th excited states, respectively.

and $2^1\Sigma_u^+$ states are, mainly, combinations of the configurations $(1\sigma_g)^1(1\sigma_u)^1$ and $(1\sigma_g)^1(2\sigma_u)^1$, while the $3^1\Sigma_u^+$ and $4^1\Sigma_u^+$ states correspond, at equilibrium distance, to the configurations $(1\sigma_g)^1(3\sigma_u)^1$ and $(1\sigma_g)^1(4\sigma_u)^1$, respectively. We are describing the composition of the excited states in terms of the familiar HF orbital based configurations. The NOs are numbered by decreasing occupation number, and NOs with high number may be important in low-lying excited states, see, e.g., Table IV of Ref. 4. The composition of the NOs in terms of the HF orbitals can be used to make the necessary identification of the type of excited state. Here we do this directly with the HF orbitals since the CI on HF orbital basis is available. Note however that the crucial $1\sigma_u$ orbital, involved in the static correlation in H_2 at stretched bond lengths, has the largest occupation of the virtual orbitals and is also the "lumo" (orbital $h + 1$) in the NO basis.

Upon bond stretching there is increasing double-excitation character (to the $(1\sigma_u)^2$ configuration) in the ground state $1^1\Sigma_g^+$ (see Sec. VI on the $^1\Sigma_g^+$ states) which leads to changes in the composition of the excited states. For instance, while in the Σ_u^+ symmetry, around R(H–H)=5 a.u. the configuration of the lowest excited $1^1\Sigma_u^+$ state is $(1\sigma_g)^1(1\sigma_u)^1$ also at elongated distances, the next states, $2^1\Sigma_u^+$ and $3^1\Sigma_u^+$, obtain at that distance strong admixtures of (off-diagonal) doubly excited configurations. The $2^1\Sigma_u^+$ retains 50% $(1\sigma_g)^1(2\sigma_u)^1$ and acquires 31% of the off-diagonal doubly excited $(1\sigma_u)^1(2\sigma_g)^1$. The $3^1\Sigma_u^+$ acquires 40% of the single excitation $(1\sigma_g)^1(2\sigma_u)^1$ and 37% of the off-diagonal double excitation $(1\sigma_u)^1(3\sigma_g)^1$. The $4^1\Sigma_u^+$ excited state becomes even predominantly doubly excited, namely, a mixture of the off-diagonal doubly excited configurations $(1\sigma_u)^1(3\sigma_g)^1$ (48%) and $(1\sigma_u)^1(2\sigma_g)^1$ (14%). Note that in all these cases the off-diagonal doubly excited configurations may also be interpreted as single excitations from the $(1\sigma_u)^2$ configuration which contributes strongly to the ground state because of the nondynamical correlation.

The results of the calculations for the lowest four $^1\Sigma_u^+$ states are shown in Fig. 1. The TDDFT calculation (not shown in the figure) for the lowest $^1\Sigma_u^+$ state shows the familiar TDDFT failure[6,7] of going steeply to zero at long R. In this case the TDDFT zero-order estimate $\omega_\alpha^s = \epsilon(1\sigma_u) - \epsilon(1\sigma_g)$, the difference between the energies of the antibonding and bonding KS orbitals, vanishes with R(H–H). In order to compensate this vanishing, the xc kernel f_{xc} of TDDFT should diverge.[6] However, the functions f_{xc} of ALDA and AGGAs remain finite in this case. As a result, the TDDFT excitation energy vanishes for larger bond distances and the corresponding potential curve does not exhibit a minimum (see Fig. 1 and Ref. 7).

The novel features of Fig. 1 are the potential curves obtained with the restricted response calculations (see Sec. IV) with the PILS functional. The calculations are performed in the same aug-cc-pVTZ basis[35] as the reference FCI ones. For each excited state the dots show the curve obtained with the response vector restricted to occ. $\rightarrow$ all $\Delta\gamma_{ia}^R$ elements, $i \leq N$, $a \in$ all (the $\Delta\gamma_{pp}^R = \Delta n_p$, all p, are always included). These are calculations of TDDFT like size of the secular

problem, which we denote R0. Unlike TDDFT, the PINO response calculations properly describe the ionic nature of the $1^1\Sigma_u^+$ and $2^1\Sigma_u^+$ states of H_2 at the distance regime in Fig. 1, producing finite and sizable excitation energies at larger R(H–H). The TDDFT catastrophe of zero excitation energies at large R has disappeared. It is remarkable that the higher excited states (already $2^1\Sigma_u^+$ but notably $3^1\Sigma_u^+$ and $4^1\Sigma_u^+$) show much poorer performance for the R0 type calculations. This is a simple consequence of the fact that those excited states have large doubly excited character, to the $(1\sigma_u)^1(2\sigma_g)^1$ for the $2^1\Sigma_u^+$, to the $(1\sigma_u)^1(3\sigma_g)^1$ configuration for $3^1\Sigma_u^+$ and to $(1\sigma_u)^1(3\sigma_g)^1$ and $(1\sigma_u)^1(2\sigma_g)^1$ for $4^1\Sigma_u^+$. For the same reason the TDDFT curves for these states are very poor.[3] Just going to the R1 variant, with only the $1\sigma_u$ "lumo" included in the range for the i index, as expected completely remedies the deficiency of the R0 type calculation, as is evident from the dot-dashed curves in Fig. 1. Further, but much less striking, improvement is obtained by adding one more orbital to the "occupied" range (R2 variant, dashes). It is clear that the primary improvement afforded by the TD-DMFT method comes from the possibility to incorporate the effect of the strong nondynamical correlation by allowing excitations out of the $(1\sigma_u)^2$ configuration which participates strongly in the ground state. The need for such an extension can be observed immediately from the abnormally high occupation number (for a "virtual" orbital) of this orbital when the nondynamical correlation is strong.

At shorter distances, one can notice a very good performance of the PINO response calculations in all R variants. Already PILS-R0 produces reasonable ω_α at shorter separations R(H–H) ≤ 3 a.u. This is understandable, since this basic variant includes single excitations, which are dominant at those distances. They are markedly improved over the TDDFT calculations. In particular the higher excited states give poor TDDFT results (see Ref. 3), whereas the R0 results are already very good. In the R2 variant the results become extremely accurate for all states except $1^1\Sigma_u^+$.

To provide a more quantitative information on the excitation energies in "normal" single reference situations, Table I displays ω_α values calculated for the equilibrium bond distance R(H–H) $= 1.401$ a.u. for the R0, R1, and R2 variants. In the R2 variant the elements of the R1 variant are further augmented with the elements $\delta\gamma_{3,a}$ between the third (homo+2) and higher NOs. One can see from Table I that there is a consistent overestimation of the excitation energies in the restricted PILS calculations, which gradually decreases when going from PILS-R0 to PILS-R1 to PILS-R2. An interesting observation is that each restricted variant is characterized with its own, nearly monotonic upward shift of all

excitation energies from the reference CI ones. Indeed, the PILS-R0 energies exhibit the largest such shift of $\sim$0.04 a.u. This shift is reduced to $\sim$0.03 a.u. for the PILS-R1 energies. Further extension from R1 to R2 removes the largest part of the remaining discrepancy and the PILS-R2 energies reproduce rather quantitatively the FCI reference with the upward shift of only 0.006 a.u. (see Table I).

We finally note that the DMLS functional (no results shown), mentioned at the end of Sec. IV, in spite of being a proper 1RDM functional with invariance with respect to the NO phases, is prone in some regions to an erratic description of excited states with our limited (R0–R2) schemes. The deficiency of the DMLS functional becomes much more pronounced when the calculations are further extended. Upon extending the range of the i index to all basis functions, the calculated spectrum exhibits very many spurious excitations that behave erratically as a function of the distance.[27]

VI. APPLICATIONS: POTENTIAL ENERGY CURVES FOR THE $^1\Sigma_g^+$ EXCITED STATES OF H_2

In this section, we proceed with the H_2 potential energy curves for the lowest states of the $^1\Sigma_g^+$ symmetry displayed in Fig. 2. Just as the $^1\Sigma_u^+$ states discussed in Sec. V, the lowest $^1\Sigma_g^+$ excited states have single-excitation character near the equilibrium distance. In the representation of the HF orbitals, the $n^1\Sigma_g^+$ states, $n = 2\ldots5$, of Fig. 2 correspond to the single-electron promotions $1\sigma_g \to n\sigma_g$ from the $1\sigma_g$ orbital to the higher $n\sigma_g$ Rydberg-like orbital of the same symmetry. The $5^1\Sigma_g^+$ state has mixed character at R_e, the largest contributions being 27% and 19% from the $(2\sigma_u)^2$ and $(1\sigma_g)^1(5\sigma_g)^1$ configurations, respectively.

With the bond stretching, the single excitation $1\sigma_g \to 2\sigma_g$ character is transferred from the lowest excited state,

TABLE I. Excitation energies (in hartree) for 4 lowest $^1\Sigma_u^+$ states of the H_2 molecule at the equilibrium bond distance.

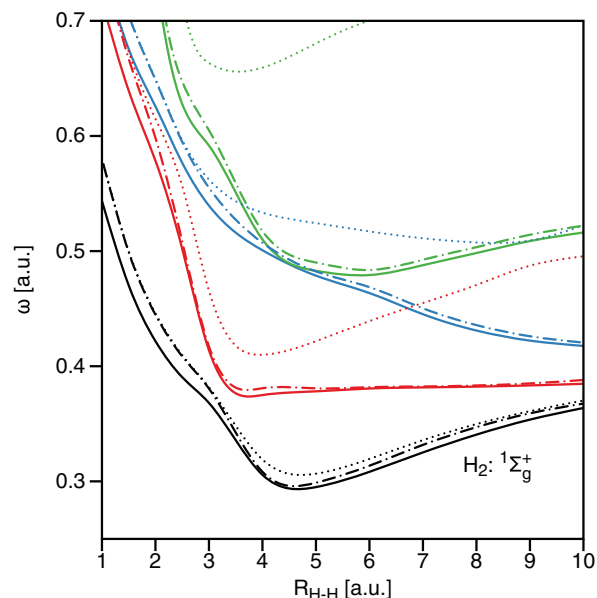| State	$1^1\Sigma_u^+$	$2^1\Sigma_u^+$	$3^1\Sigma_u^+$	$4^1\Sigma_u^+$
PILS-R0	0.506	0.614	0.816	0.920
PILS-R1	0.499	0.608	0.814	0.911
PILS-R2	0.474	0.584	0.789	0.890
FCI	0.468	0.578	0.784	0.882

FIG. 2. Exact and PILS calculations of H_2 $^1\Sigma_g^+$ excitation energies along the bond breaking coordinate. Full CI: solid lines; PILS-R0: dots; PILS-R1: dotted-dashed lines. Black, red, blue, green: $2^1\Sigma_g^+$, $3^1\Sigma_g^+$, $4^1\Sigma_g^+$, and $5^1\Sigma_g^+$ excited states, respectively.

$2^1\Sigma_g^+$ ($EF\,^1\Sigma_g^+$ in spectroscopic notation) to the next state, $3^1\Sigma_g^+$ ($H\bar{H}\,^1\Sigma_g^+$), through their avoided crossing at R(H–H) around 3 a.u. (see Fig. 2). The lowest excited state, $2^1\Sigma_g^+$, then acquires double-excitation character to $(1\sigma_u)^2$. This double excitation character is at much higher energies at shorter bond distances, see Fig. 2(b) of Ref. 3. Around 5 a.u. $2^1\Sigma_g^+$ becomes mainly the plus combination of the ground state configuration $(1\sigma_g)^2$ and the diagonal double excitation $(1\sigma_u)^2$, with comparable weights. It is elementary to show that this plus combination leads to ionic nature of the $2^1\Sigma_g^+$ state (just as the minus combination gives the covalent Heitler-London configuration in the ground state, $1^1\Sigma_g^+$). Asymptotically, the $2^1\Sigma_g^+$ state therefore tends to similar energy as the similarly ionic $2^1\Sigma_u^+$ state in Fig. 1, at least in the distance regime shown in the plots (note that at longer distance the $2^1\Sigma_g^+$ and $1^1\Sigma_u^+$ become covalent again, going to symmetry combinations of H($1s$)H($2s, 2p$) atomic states.[37]

After the avoided crossing of the next two states, $3^1\Sigma_g^+$ and $4^1\Sigma_g^+$, near R(H–H)=4.5 a.u. (see Fig. 2), the lower $3^1\Sigma_g^+$ state has at 5 bohr 62% of the singly excited $(1\sigma_g)^1(2\sigma_g)^1$ configuration and acquires 12% of the diagonal $(1\sigma_u)^2$ and 7% of the off-diagonal $(1\sigma_u)^1(2\sigma_u)^1$ doubly excited configuration. It will ultimately tend to one of the covalent states with one atom in a $1s \rightarrow 2s, 2p$ excited state, the other one in the ground state. The higher $4^1\Sigma_g^+$ state acquires 46% of the off-diagonal doubly excited $(1\sigma_u)^1(2\sigma_u)^1$ configuration, in addition to 25% of the singly excited $(1\sigma_g)^1(4\sigma_g)^1$ configuration. The $5^1\Sigma_g^+$ state has at 5 bohr 72% of the singly excited $(1\sigma_g)^1(3\sigma_g)^1$ configuration and acquires 7% of the diagonal $(1\sigma_u)^2$ and 6% of the off-diagonal $(1\sigma_u)^1(3\sigma_u)^1$ doubly excited configurations. Note, that the $2^1\Sigma_g^+$ state of the stretched H$_2$ is a striking example of excited states, which are missed in adiabatic TDDFT.[3] It is instructive to realize, that even the lowest excited state of this prototype two-electron bond molecule is missed in standard TDDFT, because it has double-excitation character. The underlying reason of this TDDFT failure is the single-excitation structure of the TDDFT density response discussed in the Introduction.

It is an important virtue of the present adiabatic PINO theory, that it reproduces the entire $2^1\Sigma_g^+$ potential energy curve along with those of other low-lying doubly excited states. Already, the basic PILS-R0 reproduces reasonably well the reference FCI curve for the lowest $2^1\Sigma_g^+$ excited state, $2^1\Sigma_g^+$, and PILS-R1 further improves the calculated excitation energy, especially, in the interval of 4–5.5 a.u. (see Fig. 2). It is striking that the "TDDFT-like" R0 variant is still rather bad for the $3^1\Sigma_g^+$, $4^1\Sigma_g^+$ and particularly $5^1\Sigma_g^+$ states, although this poor behavior is immediately remedied if one goes to the only slightly more expensive R1 variant. This behavior is again easily explained from the compositions of the excited states. At longer distances the higher excited states $3^1\Sigma_g^+ - 5^1\Sigma_g^+$ acquire increasing doubly excited character. The $3^1\Sigma_g^+$ state has at 5 a.u. 62% of the singly excited $(1\sigma_g)^1(2\sigma_g)^1$ configuration and acquires 12% of the diagonal $(1\sigma_u)^2$ and 7% of the off-diagonal $(1\sigma_u)^1(2\sigma_u)^1$ doubly excited configuration. The $4^1\Sigma_g^+$ state retains 25% of the singly excited $(1\sigma_g)^1(4\sigma_g)^1$ configuration and acquires 46% of the

TABLE II. Excitation energies (in hartree) for 4 lowest $^1\Sigma_g^+$ states of the H$_2$ molecule at the equilibrium bond distance, using the restricted variants (R0–R2) of the PINO response calculations.

State	$2^1\Sigma_g^+$	$3^1\Sigma_g^+$	$4^1\Sigma_g^+$	$5^1\Sigma_g^+$
PILS-R0	0.513	0.687	0.719	1.157
PILS-R1	0.513	0.682	0.719	1.071
PILS-R2	0.486	0.656	0.694	1.064
FCI	0.483	0.653	0.688	1.039

off-diagonal doubly excited $(1\sigma_u)^1(2\sigma_u)^1$ configuration. The $5^1\Sigma_g^+$ state retains 72% of the singly excited $(1\sigma_g)^1(3\sigma_g)^1$ configuration and acquires 7% of the diagonal $(1\sigma_u)^2$ and 6% of the off-diagonal $(1\sigma_u)^1(3\sigma_u)^1$ doubly excited configurations. We note from these compositions that the R1 variant, allowing the configurations with one occupied $1\sigma_u$ orbital ("single excitation out of $1\sigma_u$") plus of course the diagonal doubles, should perform well, and indeed it does. We note that the TDDFT calculations for these higher excited states go totally astray, see Fig. 2 in Ref. 4, in agreement with the (diagonal and off-diagonal) double excitation character of these states.

In Table II the excitation energies of the $^1\Sigma_g^+$ states calculated at the equilibrium bond distance are presented. Again, the restricted PILS calculation consistently overestimate ω_α. Note, that PILS-R1 has nearly the same almost uniform upward shift of 0.03 a.u. of its energies as for the $^1\Sigma_u^+$ states of Sec. V. PILS-R0 produces, basically, the same energies of the first three excited states as PILS-R1, while the error of the calculated $5^1\Sigma_g^+$ state appreciably decreases from PILS-R0 to PILS-R1. In its turn, the extended PILS-R2 variant produces rather quantitative agreement with FCI for the first three states and a somewhat worse quality for the fourth state, $5^1\Sigma_g^+$ (See Table II).

We finally note that again the calculations with the DMLS functional (not shown) give rather poor results. In particular, there is no DMLS excitation corresponding to the lowest FCI or PILS excitations for R(H–H) > 3 a.u. This is because DMLS has the fundamental deficiency that, as a genuine 1RDM functional, it is not able in the adiabatic approximation to produce the nonzero δn_k at finite ω, so that it cannot describe the $2^1\Sigma_g^+$ of the stretched H$_2$ with its predominantly diagonal doubly excited character.

VII. APPLICATIONS: POTENTIAL ENERGY CURVES FOR THE $^1\Sigma^+$ EXCITED STATES OF HeH$^+$

The potential energy curves for the lowest excited states of the $^1\Sigma^+$ symmetry of the HeH$^+$ molecule are displayed in Fig. 3. HeH$^+$ is an example of a simple molecular system with CT excitations. Unlike the excitations in the H$_2$ molecule discussed in Secs. V and VI, the lowest excitations in HeH$^+$ are, mainly, single excitations at all bond distances. Excitations in the stretched HeH$^+$ molecule can be described as combinations of the long-range CT of a single electron from He to H and a single-electron promotion to the higher, Rydberg-like orbitals of He.
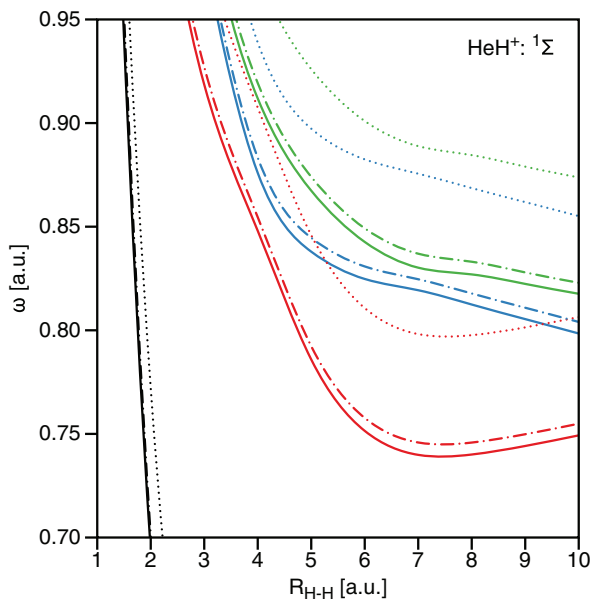
FIG. 3. Exact and PILS calculations of HeH^+ $^1\Sigma^+$ excitation energies to the 1st–4th excited states along the bond breaking coordinate. FCI: solid lines; PILS-R0: dots; PILS-R1: dotted-dashed lines. Black, red, blue, green: 1st–4th excited state, $2^1\Sigma^+$–$5^1\Sigma^+$.

TABLE III. Excitation energies (in hartree) for lowest 4 $^1\Sigma^+$ states of the HeH^+ molecule at the equilibrium bond distance.

State	$2^1\Sigma^+$	$3^1\Sigma^+$	$4^1\Sigma^+$	$5^1\Sigma^+$
PILS-R0	1.027	1.275	1.433	1.506
PILS-R1	0.977	1.242	1.397	1.472
PILS-R2	0.973	1.230	1.388	1.461
FCI	0.964	1.225	1.383	1.456

ory accurately describes the dynamics of two-electron systems (see Sec. II). Then, deviations of the PILS curves in Figures 1–3 are solely due to a limited number of $\delta\gamma_{kl}$ elements retained in the restricted variants PILS-R0 and PILS-R1. It appears that the effect of restriction of the response vector, in particular the R0 case, are somewhat larger for HeH^+, while an apparent cause such as the nondynamical correlation in elongated H_2 is not obvious. The PILS-R0 variant consistently overestimates the excitation energy ω_α of HeH^+ by some 0.05 a.u. It is interesting to note that all PILS-R0 curves exhibit a nearly uniform upward shift of this amount at all bond distances considered (see Fig. 3). In PILS-R1 this shift is reduced by an order of magnitude for the stretched HeH^+. As can be seen in Table III the PILS-R2 variant further improves to the same level of $\sim$0.005 a.u. as in stretched H_2. Due to this, all PILS-R2 curves closely reproduce the reference FCI ones (see Fig. 3).

The DMLS-R1 curves (not shown) are reasonable in this case. One can attribute this to the predominantly single-excitation nature of the HeH^+ $^1\Sigma^+$ states. Also for $^1\Sigma_u^+$ and $^1\Sigma_g^+$ states of H_2 we have observed relatively reasonable results with DMLS-R1 for excited states with very little double excitation character. Apparently, DMLS-R1 performs better for the mostly single-excitation states, such as the present excited $^1\Sigma^+$ states of HeH^+. Again, however, the DMLS calculations deteriorate upon extension of the response vector.

In Table III the excitation energies of the $^1\Sigma^+$ states calculated at the equilibrium He–H^+ bond distance are presented. One can see in Table III the above mentioned nearly consistent overestimation of the excitation energies with the restricted PILS-R0 calculations, which is close to 0.05 a.u. at the equilibrium distance. In PILS-R1 this shift is reduced to $\sim$0.015 a.u., which is only half the corresponding PILS-R1 shift for excitations in H_2 (see Tables I and II). Again, extension to PILS-R2 substantially reduces the upward shift and produces a rather quantitative agreement with FCI.

VIII. CONCLUSIONS

In this paper the orbital excitation structure of the 1RDM response is analyzed and the adiabatic response PINO theory is applied to the calculation of the energies of bonding $\rightarrow$ antibonding (bond breaking) excitations, double excitations (both diagonal and off-diagonal), high (including Rydberg-type) excitations, and (pseudo) charge transfer excitations, along the bond-dissociation coordinate of the prototype molecules H_2 and HeH^+.

The interpretation of the 1RDM response in terms of the transition density matrices associated with the excited

The lowest $2^1\Sigma^+$ excited state of stretched HeH^+ has a significantly lower energy than other states. Its PES goes down to $\sim$0.40 a.u. and then becomes flat. It represents a relatively low-energy CT from the 1s orbital of He to the 1s orbital of H, which no longer changes in energy beyond $\sim$4.5 bohr. In Fig. 3 only part of the curve for this state is visible, in order to display the more interesting higher states better. The $2^1\Sigma^+$ excited state is described excellently at the PILS-R1 level along the entire distance range, and even the R0 approximation is not so bad, just being some 0.05 a.u. too high in the asymptotic distance range. The next state, $3^1\Sigma^+$, is at $R(\text{He-H}) = 5$ a.u. a mixture of the CT (which has a larger contribution) to, mainly, the $2p_z$ orbital of H (z is the molecular axis) plus a local excitation He(1s) $\rightarrow$ He(2s). The $4^1\Sigma^+$ is mostly CT, He(1s) $\rightarrow$ H(2s, 2p). And the $5^1\Sigma^+$ is, again, a mixture of a local excitation (which has, this time, a larger contribution) He(1s) $\rightarrow$ He(2s) plus the CT He(1s) $\rightarrow$ H(2s).

As was mentioned in the Introduction, the long-range CT presents a problem in TDDFT.[8,14] In the case of a donor-acceptor CT excitation, in order to provide the proper correction to the deficient zero-order TDDFT estimate $\omega_\alpha^s = \epsilon_a - \epsilon_i$, the xc kernel f_{xc} should diverge in the long-range limit.[12] However, the present CT to the zero-electron acceptor H^+, as was explained in Ref. 4, is a special case, in which the accurate ω_α^s of the KS theory would be also the accurate long-range CT excitation energy ω_α. In this case, the substantial underestimation of the HeH^+ excitation energy observed in Ref. 4 with the standard ALDA and AGGAs of TDDFT, is due to the underestimation of the donor ionization energy (1s orbital energy) with these approximations, which becomes particularly large for He.

In contrast, PILS is an accurate functional for stationary two-electron systems. Moreover, adiabatic PINO-PILS the-

states is derived. It is emphasized that the 1RDM response encompasses both single and double excitation character of transitions to the excited states. Restricted variants of the response calculations are proposed, in which the size of the response vector is effectively reduced by retaining only single excitation as well as diagonal and a limited number of off-diagonal double-excitation 1RDM response elements. It proves to be possible to reduce the size of the density matrix response problem, which in principle has dimension of the order $\frac{1}{2}n^2 \times \frac{1}{2}n^2$ with n the number of basis functions, to dimensions only slightly larger than the $n_{occ}n_{virt} \times n_{occ}n_{virt}$ size of TDDFT response calculations.

The restricted adiabatic PINO theory is shown to successfully resolve problematic cases of adiabatic TDDFT. Adiabatic time-dependent PINO theory can naturally describe double excitations, which are absent in the adiabatic TDDFT. The PINO theory also successfully resolves the problem of standard TDDFT of the vanishing energy of the bond-breaking $(\sigma_g \rightarrow \sigma_u)$ excitation to the $1\,^1\Sigma_u^+$ state of the H_2 molecule. In part of the distance range this state is strongly ionic and this transition has pseudo CT character, which does not pose any problem. The true CT transitions in the stretched HeH$^+$ molecule are also described very well. For both H_2 and HeH$^+$ the higher excited states show marked improvement when the TDDFT-like size of the problem of the R0 variant is somewhat extended in the R1 and R2 variants. These afford off-diagonal double excitations, or equivalently, in H_2, excitations out of the $1\sigma_u$ orbital, which becomes fractionally occupied at long distances. At the moderately extended PILS-R2 level rather quantitative agreement with the reference FCI data is obtained.

We have shown that it is important to extend TDDMFT to include further parameters, which enter the theory as phases of the orbitals.[25,26] This leads to the PINO response theory applied in this work. The present results manifest the crucial importance of using in the adiabatic approach of time-dependent theory orbital functionals with the proper orbital phase dependence. It appears that, unlike the PINO-PILS response calculations, the TDDMFT calculations with the density matrix functional DMLS (orbital phase invariant) fail to treat properly double excitations. Because of this, the restricted DMLS-R1 misses the lowest excited $^1\Sigma_g^+$ state of the stretched H_2 which has diagonal double-excitation character. It also produces a too low-lying artificial intruder $^1\Sigma_u^+$ state of H_2 at shorter bond distances. As a matter of fact, the DMLS calculations are not stable against further extension of the size of the response problem. Upon extending the range of the i index to all basis functions, the calculated spectrum then becomes totally unrealistic, with very many spurious excitations that behave erratically as a function of the distance.[27]

The natural next step of the development of the PINO theory would be application of this theory to the adiabatic response calculations of systems having more than two electrons. For this, the development of an N-electron functional is required, which, just as the two-electron PILS functional of the present paper, would have a proper dependence on PINOs and would provide a good quality of the potential energy curves for excited states obtained with, preferably, similarly restricted calculations as explored in this paper. This work is in progress.

[1]N. T. Maitra, F. Zhang, R. J. Cave, and K. Burke, J. Chem. Phys. **120**, 5932 (2004).
[2]J. Neugebauer and E. J. Baerends, J. Chem. Phys. **121**, 6155 (2004).
[3]K. J. H. Giesbertz, E. J. Baerends, and O. V. Gritsenko, Phys. Rev. Lett. **101**, 033004 (2008).
[4]K. J. H. Giesbertz, K. Pernal, O. V. Gritsenko, and E. J. Baerends, J. Chem. Phys. **130**, 114104 (2009).
[5]I. A. Mikhailov, S. Tafur, and A. Masunov, Phys. Rev. A **77**, 012510 (2008).
[6]O. Gritsenko, S. J. A. van Gisbergen, A. Görling, and E. J. Baerends, J. Chem. Phys. **113**, 8478 (2000).
[7]K. J. H. Giesbertz and E. J. Baerends, Chem. Phys. Lett. **461**, 338 (2008).
[8]A. Dreuw, J. L. Weisman, and M. Head-Gordon, J. Chem. Phys. **119**, 2943 (2003).
[9]K. Pernal, O. Gritsenko, and E. J. Baerends, Phys. Rev. A **75**, 012506 (2007).
[10]K. Pernal, K. Giesbertz, O. Gritsenko, and E. J. Baerends, J. Chem. Phys. **127**, 214101 (2007).
[11]M. E. Casida, in *Recent Advances in Density-Functional Methods, Part I*, edited by D. P. Chong (World Scientific, Singapore, 1995), p. 155
[12]O. Gritsenko and E. J. Baerends, J. Chem. Phys. **121**, 655 (2004).
[13]O. Gritsenko and E. J. Baerends, Can. J. Chem. **87**, 1383 (2009).
[14]A. Dreuw and M. Head-Gordon, Chem. Rev. **105**, 4009 (2005).
[15]M. Hellgren and E. K. U. Gross, e-print arXiv:1108.3100.v1.
[16]O. V. Gritsenko, K. Pernal, and E. J. Baerends, J. Chem. Phys. **122**, 204102 (2005).
[17]M. Piris, Int. J. Quantum Chem. **106**, 1093 (2006).
[18]N. N. Lathiotakis and M. Q. L. Marques, J. Chem. Phys. **128**, 184103 (2008).
[19]M. A. L. Marques and N. N. Lathiotakis, Phys. Rev. A **77**, 032509 (2008).
[20]N. N. Lathiotakis, N. Helbig, A. Zacarias, and E. K. U. Gross, J. Chem. Phys. **130**, 064109 (2009).
[21]D. R. Rohr, K. Pernal, O. V. Gritsenko, and E. J. Baerends, J. Chem. Phys. **129**, 164105 (2008).
[22]M. Piris, X. Lopez, F. Ruipérez, J. M. Matxain, and J. M. Ugalde, J. Chem. Phys. **134**, 164102 (2011).
[23]H. Appel and E. K. U. Gross, Europhys. Lett. **92**, 23001 (2010).
[24]R. Requist and O. Pankratov, Phys. Rev. A **83**, 052510 (2011).
[25]K. J. H. Giesbertz, O. V. Gritsenko, and E. J. Baerends, Phys. Rev. Lett. **105**, 013002 (2010).
[26]K. J. H. Giesbertz, O. V. Gritsenko, and E. J. Baerends, J. Chem. Phys. **133**, 174119 (2010).
[27]K. J. H. Giesbertz, "Time-dependent one-body reduced density matrix functional theory; adiabatic approximations and beyond," Ph.D. dissertation (Vrije Universiteit, 2010)
[28]E. Runge and E. K. U. Gross, Phys. Rev. Lett. **52**, 997 (1984).
[29]G. Vignale, Phys. Rev. A **77**, 062511 (2008).
[30]Note that we assumed here that the A^+ is positive definite. If the ground state has been taken as the reference state, this is indeed the case, since the matrix A^+ can be identified with the PINO Hessian (see Ref. 27).
[31]A. L. Fetter and J. D. Walecka, *Quantum Theory of Many-Particle Systems* (Dover, New York, 2003)
[32]A. M. K. Müller, Phys. Lett. A **105**, 446 (1984).
[33]M. Buijse, "Electron correlation," Ph.D. dissertation (Vrije Universiteit, 1991)
[34]M. Buijse and E. J. Baerends, Mol. Phys. **100**, 401 (2002).
[35]T. H. Dunning, Jr., J. Chem. Phys. **90**, 1007 (1989).
[36]O. Christiansen, A. Halkier, H. Koch, P. Jørgensen, and T. Helgaker, J. Chem. Phys. **108**, 2801 (1998).
[37]J. Wang, K. S. Kim, and E. J. Baerends, J. Chem. Phys. **135**, 074111 (2011).